1-1-2005

# Novel Cyanine-AMP Conjugates for Efficient 5' RNA Fluorescent Labeling by One-Step Transcription and Replacement of [Î³-$^{32}$P] ATP in RNA Structural Investigation

Na Li
*University of Southern Mississippi*

Changjun Yu
*AdeGenix, Inc.*

Faqing Huang
*University of Southern Mississippi*, Faqing.Huang@usm.edu

Published online February 24, 2005

*Nucleic Acids Research, 2005, Vol. 33, No. 4* ***e37***
*doi:10.1093/nar/gni036*

# Novel cyanine-AMP conjugates for efficient 5′ RNA fluorescent labeling by one-step transcription and replacement of [γ-$^{32}$P]ATP in RNA structural investigation

**Na Li, Changjun Yu[1] and Faqing Huang***

Department of Chemistry and Biochemistry, University of Southern Mississippi Hattiesburg, MS 39406-5043, USA and [1]AdeGenix, Inc., 870 S. Myrtle Avenue, Monrovia, CA 91016, USA

Received November 23, 2004; Revised and Accepted February 4, 2005

## ABSTRACT

**Two novel fluorescent cyanine-AMP conjugates, F550/570 and F650/670, have been synthesized to serve as transcription initiators under the T7 ϕ2.5 promoter. Efficient fluorophore labeling of 5′ RNA is achieved in a single transcription step by including F550/570 and F650/670 in the transcription solution. The current work makes fluorescently labeled RNA readily available for broad applications in biochemistry, molecular biology, structural biology and biomedicine. In particular, site-specifically fluorophore-labeled large RNAs prepared by the current method may be used to investigate RNA structure, folding and mechanism by various fluorescence techniques. In addition, F550/570 and F650/670 may replace [γ-$^{32}$P]ATP to prepare 5′ labeled RNA for RNA structural and functional investigation, thereby eliminating the need for the unstable and radio-hazardous [γ-$^{32}$P]ATP.**

## INTRODUCTION

Site-specific fluorescent labeling of RNA has many applications in biochemistry, molecular biology, structural biology and biomedicine (1–15). Fluorophores may be attached to RNA either by phosphoramidite chemistry during RNA synthesis (1–3,16), post-transcriptional fluorophore coupling with enzymatically prepared RNA (16,17), or direct fluorophore labeling during transcription (18,19). Phosphoramidite chemistry-based fluorescent labeling is commonly used to synthesize relatively small RNA molecules (<50–60 nt). When the size of RNA increases, such fluorescent-labeling procedures become impractical due to low yields of full-length RNA, high levels of impurities with short RNA fragments and high costs of chemical synthesis. On the other hand, transcription-based RNA synthesis and fluorescent labeling has no apparent RNA size restrictions; both purities and costs are essentially independent of RNA sizes. Post-transcriptional fluorescent labeling involves two essential steps: preparation of amino- or thio-derivatized RNA by transcription followed by fluorophore coupling via fluorophore-*N*-hydroxysuccinimide esters (NHS) or fluorophore-maleimides or fluorophore-bromides (16,17). The limitations of this method lie in (i) the scarcity of available amino- and thio-nucleotide precursors for the preparation of amino- and thio-derivatized RNA, respectively; (ii) the hydrolytic lability of fluorophore-NHS; (iii) high concentrations of fluorophore-NHS, fluorophore-maleimides or fluorophore-bromides that are required to achieve efficient fluorescent labeling of RNA; and (iv) multiple steps of manipulation of RNA samples, leading to laborious sample preparation and low RNA yields.

Direct RNA labeling at the 5′ end using the T7 ϕ2.5 promoter developed in our laboratory (18,19) only requires appropriate label-linker-AMP conjugates (adenosine 5′-monophosphate, AMP) to serve as transcription initiators. The newly developed *in vitro* transcription system recognizes the adenosine moiety and labels the 5′ end of RNA with high efficiency through transcription initiation (18,19). The only RNA sequence requirement is the 5′ AG. We have previously reported fluorescein-HDA-AMP (1,6-hexanediamine, HDA) for direct RNA labeling (19). For this new RNA-labeling method to be widely applicable, however, diverse fluorophores with better spectroscopic properties, such as the commonly used cyanine dye family, are highly desirable. Here, we describe the synthesis of two novel cyanine-AMP conjugates, **F550/570** and **F650/670**, and their use to fluorescently label 5′ RNA in a single transcription step. Furthermore, we demonstrate one utility, among others, of **F550/570** to replace the commonly used [γ-$^{32}$P]ATP for 5′ RNA labeling in RNA structure/function/mechanism investigation.

*To whom correspondence should be addressed. Tel: +1 601 266 4371; Fax: +1 601 266 6075; Email: faqing.h.huang@usm.edu

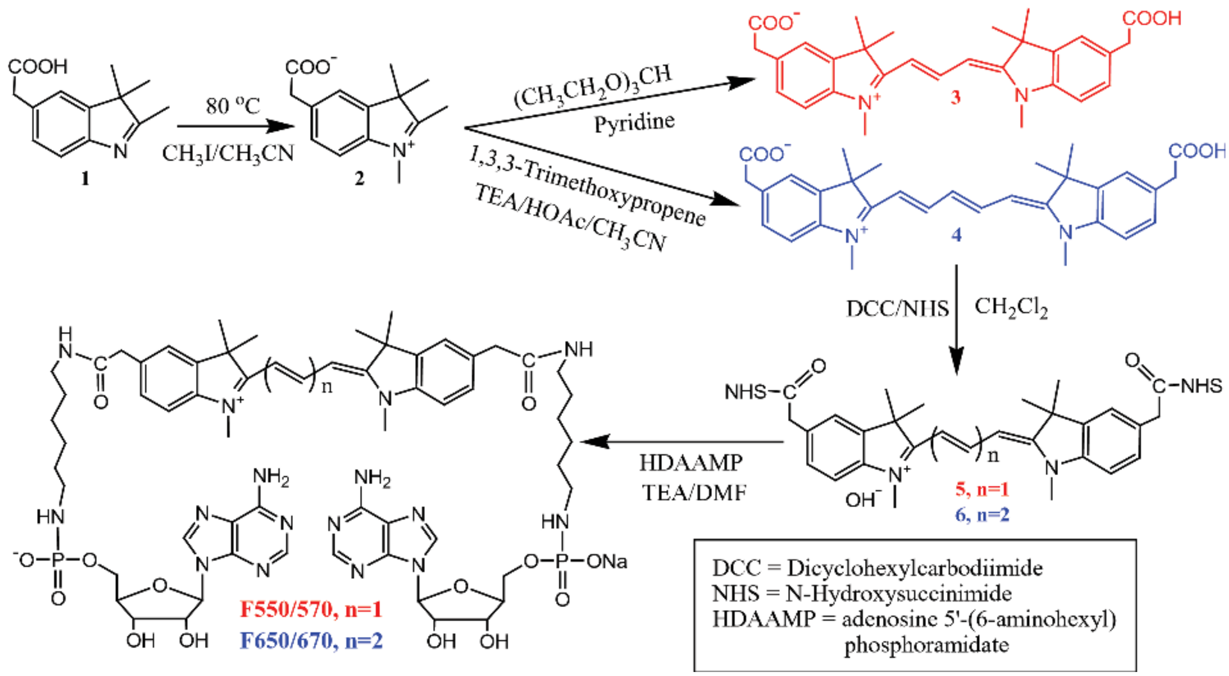


**Scheme 1.** Synthesis of cyanine-AMP conjugates.

## MATERIALS AND METHODS

### Synthesis of cyanine-AMP conjugates

All reagents and chemicals were purchased from Aldrich and used as received. Synthetic procedures are shown in Scheme 1. Starting from 2,3,3-trimethyl-3H-indole-5-acetic acid **1** (20), the common intermediate 1,2,3,3-tetramethyl-indoleninium-5-acetate (2) was synthesized by methylation of **1** (20). Condensation of two molecules of **2** with one molecule of triethyl orthoformate (21) afforded the symmetrical red cyanine dye **3** with two free carboxyl groups that can be used for subsequent conjugation with AMP via a linker. Separately, condensation of one molecule of 1,3,3-triemethoxypropene (21) with two molecules of **2** produced another symmetrical blue cyanine dye **4** with two free carboxyl groups. The carboxyl groups of **3** and **4** were then activated by *N*,*N*′-dicyclohexylcarbodiimide (DCC) to form their corresponding NHS esters, **5** and **6**. Finally, the intermediates **5** and **6** were individually coupled with 5′-(6-aminohexyl) adenosine phosphoramidate (HDAAMP) (19) to afford a pair of novel symmetrical cyanine-AMP conjugates, **F550/570** and **F650/670**. Detailed description of the syntheses of **2–6, F550/570** and **F650/670** are given below.

*Synthesis of compound* **2.** To a 25 ml Schlenk tube was added 0.5 g (2.3 mmol) of compound **1**, prepared from the published procedure (20), 1.2 ml (19.3 mmol) of iodomethane and 10 ml of acetonitrile. The reaction mixture was degassed with argon for 30 min and the tube was sealed with a cap and heated in an oil bath at 80°C for 1 h. After cooling, the reaction mixture was transferred into a flask and concentrated under vacuum to give 0.78 g (94%) of product **2**.

*Synthesis of compound* **3.** The literature procedures (20,21) were used to prepare compound **3**. To 1.0 g (2.8 mmol) of compound **2**, 20 ml of dry pyridine was added. While the reaction mixture was refluxing, 1.4 ml (8.4 mmol) of triethyl orthoformate was added slowly (0.4 ml per 15 min). After completion of addition, the reaction mixture was refluxed for another 2 h. Solvent was removed and the red residue was dissolved in 40 ml of methanol, followed by adding 200 ml of ethyl acetate. After concentrating to ∼50 ml, another 100 ml of ethyl acetate was added, and concentrated to ∼50 ml. To this suspension, 100 ml of ethyl acetate was added. The top solvent was decanted and the red residue was dried over under vacuum to give 0.81 g (96%) of the compound **3**. Mass spectrometry (MS) analysis gave the following results: $C_{29}H_{33}N_2O_4^+$, calcd, 473.24, found 473.2 ($M^+$).

*Synthesis of compound* **4.** The literature procedure (21) was used to prepare compound **4**. To 1.0 g (2.8 mmol) of compound **2**, 28 ml of dry acetonitrile, 0.6 ml of triethylamine (TEA) and 0.2 ml of acetic acid were added. While the reaction mixture was refluxing, a solution of 1.0 g (7.6 mmol) of 1,3,3-trimethoxypropene in 4.0 ml of acetonitrile was slowly added (0.5 ml per 15 min). After completion of the addition, the reaction mixture was refluxed for another 2 h. Solvent was removed and the blue/purple residue was dissolved in 40 ml of methanol, followed by adding 200 ml of ethyl acetate. After concentrating to ∼50 ml, another 100 ml of ethyl acetate was added, and concentrated to ∼50 ml. To this suspension, another 100 ml of ethyl acetate was added, the top solvent was decanted and the red residue was dried over a high vacuum to give 0.84 g (96%) of the compound **4**. The molecular peak found by MS, 499.2 ($M^+$), is consistent with the expected formula $C_{31}H_{35}N_2O_4^+$, 499.26.

*Synthesis of* **5** *and* **6**. To 100 mg (0.16 mmol) of compound **3** or **4**, 90 ml of $CH_2Cl_2$, 100 mg (0.48 mmol) of DCC, 55 mg (0.48 mmol) of NHS and 50 mg of 4-(dimethylamino)pyridine were added. The reaction mixture was stirred for 2 h. The urea-derivative precipitate was formed and filtered off. The filtrate was concentrated to dryness and used for the next step of coupling reaction without further purification. MS analysis gave the following results: **5**—$C_{37}H_{39}N_4O_8^+$, calcd, 667.28, found 667.2 ($M^+$); **6**—$C_{39}H_{41}N_4O_8^+$, calcd, 693.29, found 693.2 ($M^+$).

*Synthesis and purification of **F550/570** and **F650/670***. To a 300 µl aqueous solution of 370 mM HDAAMP (19), 150 µl TEA, 750 µl *N*,*N*-dimethylformide (DMF) and 20 mg of **5** or **6**, which were dissolved separately in 150 µl DMF, were added. After 30 min of reaction, 1.2 ml of water was added to the sample. The resulting solution was filtered with a 0.2 µm syringe filter. Purification of **F550/570** and **F650/670** was achieved by semi-preparative reverse phase high-performance liquid chromatography (HPLC) (Figures 1 and 2). Isolated yields for **F550/570** and **F650/670** were ∼20%. High-resolution MS analysis gave excellent results: **F550/570**—$C_{61}H_{85}N_{16}O_{14}P_2^+$, calcd, 1327.5901, found 1327.5869 ($M^+$); **F650/670**—$C_{63}H_{87}N_{16}O_{14}P_2^+$, calcd, 1353.6057, found 1353.5998 ($M^+$).

### Spectroscopic properties of F550/570 and F650/670

UV absorbance spectra and molar extinction coefficiencies of **F550/570** and **F650/670** were obtained from a JASCO spectrometer (V-530) in 20 mM phosphate, pH 7.0. Fluorescence emission spectra were measured with an ISS PC1 fluorometer (Champaign, IL) in 20 mM phosphate, pH 7.0, under the



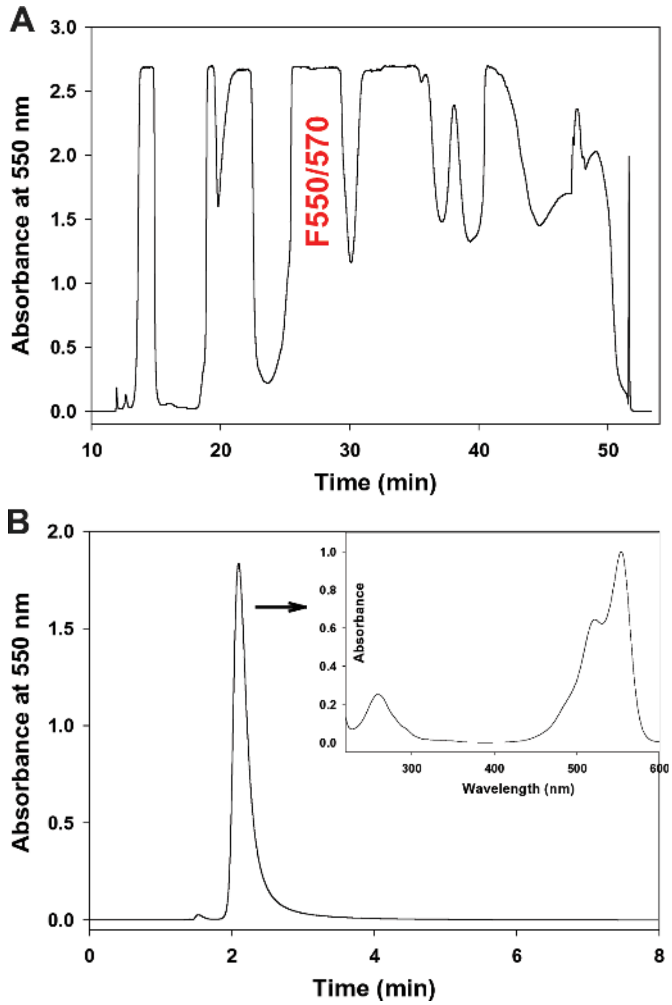


**Figure 1.** Purification and subsequent analysis of **F550/570** by HPLC. (**A**) **F550/570** sample was injected onto a Delta Pak C18 column, 7.8 × 300 mm$^2$, pre-equilibrated in 20 mM phosphate buffer, pH 7.0, flow rate 5 ml/min. The mobile phase was manually changed in the following order: 100% water at 7 min → 20% MeOH/80% water at 9 min → 30% MeOH/70% water at 16 min → 40% MeOH/60% water at 23 min → 50% MeOH/50% water at 30 min → 60% MeOH/40% water at 38 min → 100% MeOH at 45 min. The 25–30 min fraction (marked as **F550/570**) has the desired UV spectrum from an online photodiode array detector. (**B**) Analysis of the 25–30 min fraction by an Econosphere C18 column, 4.6 × 50 mm$^2$, in 60% MeOH/40% 20 mM phosphate, pH 7.0, flow rate 0.5 ml/min. The insert shows the UV–visible spectrum of the peak.

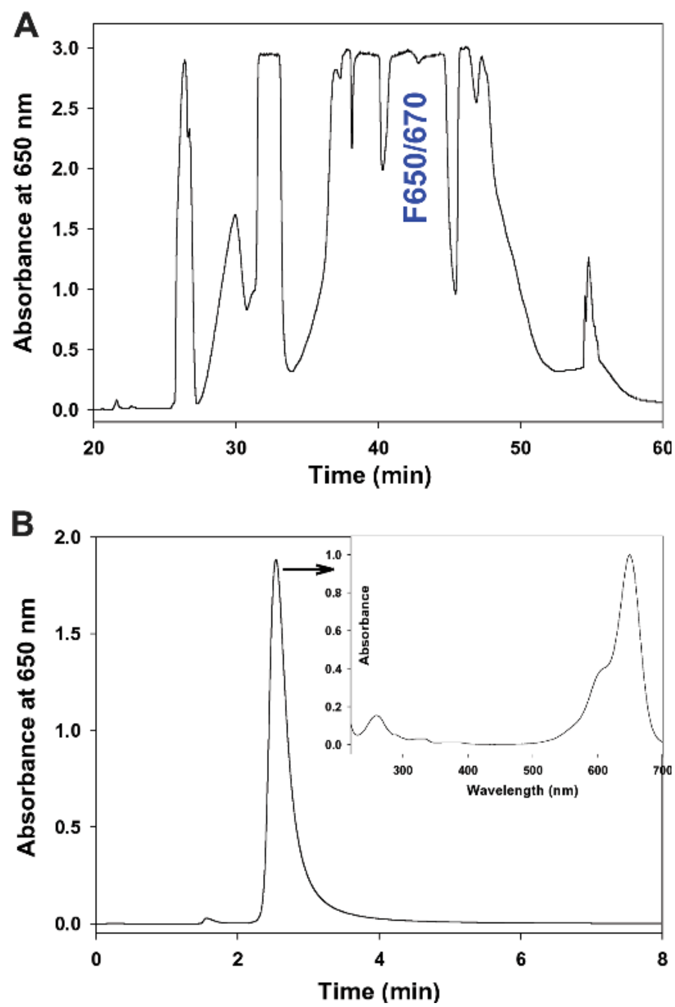


**Figure 2.** Purification and subsequent analysis of **F650/670** by HPLC. (**A**) **F650/670** sample was injected onto a Delta Pak C18 column, 7.8 × 300 mm$^2$, pre-equilibrated in 20 mM phosphate buffer, pH 7.0, flow rate 5 ml/min. The mobile phase was manually changed in the following order: 100% water at 11 min → 20% MeOH/80% water at 18 min → 30% MeOH/70% water at 23 min → 40% MeOH/60% water at 29 min → 50% MeOH/50% water at 35 min → 60% MeOH/40% water at 43 min → 100% MeOH at 52 min. The 41–45 min fraction (marked as **F650/670**) has the desired UV spectrum from an online photodiode array detector. (**B**) Analysis of the 41–45 min fraction by an Econosphere C18 column, 4.6 × 50 mm$^2$, in 60% MeOH/40% 20 mM phosphate, pH 7.0, flow rate 0.5 ml/min. The insert shows the UV–visible spectrum of the peak.

excitation of 510 and 610 nm for **F550/570** and **F650/670**, respectively. Quantum yields (Φ) of **3**, **4**, **F550/570** and **F650/670** were determined by using reference fluorophores according to the following equation:

$$\Phi_X = \Phi_R(SL_X/SL_R)(\eta_X/\eta_R)^2, \quad 1$$

where X and R stand for the sample and the reference, respectively. SL is the slope of integrated fluorescence area versus absorbance and η is the refractive index of the solvent. The reference for **3** and **F550/570** was rhodamine 101 ($\Phi_R = 1$; Fluka) (22). Zinc phthalocyanine ($\Phi_R = 0.3$; Aldrich) (23) was used as the reference for quantum-yield measurements of **4** and **F650/670**. Fluorescence was measured at the excitation of 490 nm (for **3** and **F550/570**) or 600 nm (for **4** and **F650/670**).

### RNA 5′ labeling by F550/570 and F650/670

Fluorescent labeling of 5′ RNA by **F550/570** and **F650/670** was performed under normal *in vitro* transcription conditions (18,19) with slight modifications: changing [ATP] from 1 to 0.25 mM and adding 2 mM of **F550/570** or **F650/670** to the transcription solution. The final transcription solution contained 40 mM Tris–HCl, pH 8.0, 5 mM dithiothreitol, 6 mM $MgCl_2$, 2 mM spermidine, 0.01% Triton X-100, 0.25 mM ATP, 1 mM each of UTP, GTP and CTP, 2 mM **F550/570** or **F650/670**, 0.05–0.5 μM dsDNA containing the T7 ϕ2.5 promoter (18,19), 500 U of T7 RNA polymerase per 100 μl reaction and 10–20 U of RNase inhibitor per 100 μl reaction. Also included was 2 μl of [α-$^{32}$P]ATP per 100 μl reaction as a tracer for RNA analysis. The labeling reaction was carried out at 37°C for 2 h before analysis by denaturing PAGE. Product detection and quantification were achieved by phosphorimaging/fluorimaging under the excitation by $^{32}$P, a 532 nm green laser, and a 633 nm red laser (Typhoon 9400; Amersham Biosciences). For Figure 4, the RNA was a 92-nt ribozyme (TES33) with the sequence of AGGGAAGUGCUACCACACUUGCUGGUGUACGCGCCCCCUUGCGUACUCUGCCCUUCCGCGUCUCCCCGUCCAACGGGCAUGCGGCCAGCCA, which was previously isolated in our laboratory (24). In addition, to test transcription-labeling yields and PAGE separation of varying RNA, we prepared five different RNA sizes of 100, 200, 300, 400 and 500 nt using self-constructed DNA templates from Epicentre's control DNA for AmpliScribe™ system. The sequences of transcribed RNAs are AGAAUUCUAAGCGGAGAUCGCCUAGUGAUUUUAAACUAUUGCUGGCAGCAUUCUUGAGUCCAAUAUAAAAGUAUUGUGUACCUUUUGCUGGGUCAGGUU**G**UUCUUUAGGAGGAGUAAAAGGAUCAAAUGCACUAAACGAAACUGAAACAAGCGAUCGAAAAUAUCCCUUUGGGAUUCUUGACUCGAUAAGUCUAUUAUU**U**UCAGAGAAAAAAUAUUCAUUGUUUUCUGGGUUGGUGAUUGCACCAAUCAUUCCAUUCAAAAUUGUUGUUUUACCACACCCAUUCCGCCCGAUAAAAGCA**U**GAAUGUUCGUGCUGGGCAUAGAAUUAACCGUCACCUCAAAAGGUAUAGUUAAAUCACUGAAUCCGGGAGCACUUUUUCUAUUAAAUGAAAAGUGGAAAU**C**UGACAAUUCUGGCAAACCAUUUAACACACGUGCGAACUGUCCAUGAAUUUCUGAAAGAGUUACCCCUCUAAGUAAUGAGGUGUUAAGGACGCUUUCAUU**U**, where each boldface nucleotide represents the 3′ end of an RNA sequence from the beginning A.

### Replacement of [γ-$^{32}$P]ATP by F550/F570 in RNA reaction site mapping

**F550/570**-labeled RNA (prepared as described above) was used to investigate the reaction site of an *in vitro* isolated ribozyme ACT3 that catalyzes self-aminoacylation from biocytinyl CoA (biocytinCoA) (25). Gel-purified dye-labeled ACT3 RNA was reacted for 10 min at 25°C with 1 mM biocytinCoA in the selection buffer containing 20 mM HEPES (pH 7.4), 200 mM KCl, 100 mM NaCl, 30 mM $MgCl_2$ and 10 mM $CaCl_2$ (25). After purification by membrane filtration using a microcon M30 (Millipore), the RNA was partially hydrolyzed by lead under the following conditions: 2 mM lead acetate in 7 M urea and 50 mM HEPES, pH 5.5, 40 s at 80°C, followed by quenching with 50 mM EDTA. The resultant RNA fragments were loaded onto a Neutravidin column (Pierce). Following washing with 4 M NaCl, 3 M sodium acetate and water, RNA fragments were eluted by 20 mM biotin and 5 M urea at 95°C for 10 min. The eluted RNA was EtOH-precipitated and the recovered RNA was analyzed by 8% denaturing PAGE, followed by phosphorimaging under the excitation of a 532 nm green laser.

An RNase T1 ladder of the **F550/570**-labeled RNA was prepared by digestion (10 min at 50°C) of **F550/570**-labeled RNA with 2 μg of carrier tRNA, 1 U of RNase T1 in 7 M urea, 2 mM EDTA and 0.1 M sodium acetate, pH 5.2. The ladder served as RNA size markers in RNA fragment analysis by PAGE (Figure 6B).

## RESULTS

### Synthesis of F550/570 and F650/670

Cyanine dyes (26) display some excellent fluorescent properties, including their high molar extinction coefficiencies and improved resistance to photobleaching (in contrast to the commonly used fluorescein). In addition, the color and solubility of cyanine dyes can be modulated by the number of double bonds between the two indole rings and by changing the attached chemical groups. Having successfully demonstrated 5′ fluorescein labeling of RNA by direct transcription (19), we sought to develop similar methods to site-specifically label 5′ RNA by cyanine dyes with the intention of bringing this simple and efficient RNA-labeling technique to broad applications in biosciences and biomedicine.

After two synthetic steps (Scheme 1), the two fluorescent cyanine dyes **3** and **4** were obtained in high yield (91%). After activation by DCC and NHS, the NHS esters **5** and **6** were readily coupled with the amino group of HDAAMP (19). Purification by reverse phase HPLC (Figures 1A and 2A) yielded pure (>96% purity) fluorescent dyes **F550/570** and **F650/670** (with ∼20% total yields) as shown in Figures 1B and 2B. In addition to **F550/570** and **F650/670**, there were other peaks containing cyanine dyes (Figures 1A and 2A). Their identities were not further investigated.

### UV absorbance and fluorescent properties of F550/570 and F650/670

Ultraviolet and visible spectra of **F550/570** and **F650/670** (Figure 3, Ab lines) show additive contribution from both the adenosines and the cyanine cores. For both cyanine-AMP conjugates, the absorbance within 220–300 nm is contributed mainly by the adenosine moieties. The absorbance between 450 and 580 nm of **F550/570**, with $\lambda_{max}$ at 550 nm, is purely due to the cyanine dye **3** core. Similarly, for **F650/670**, the absorbance between 580 and 700 nm ($\lambda_{max}$ = 650 nm) originates from the cyanine dye **4** core. Molar extinction coefficiencies measured in 20 mM phosphate buffer, pH 7.0, are $\varepsilon_{550} = \sim130\ 000\ M^{-1}\ cm^{-1}$ and $\varepsilon_{650} = \sim210\ 000\ M^{-1}\ cm^{-1}$ for **F550/570** and **F650/670**, respectively. Fluorescence emission spectra of **F550/570** and **F650/670** are marked as Em curves in Figure 3. **F550/570** fluoresces between 550 and 700 nm, with emission $\lambda_{max}$ = 570 nm. Under excitation, **F650/670** emits fluorescence within 640–780 nm ($\lambda_{max}$ = 670 nm). Within the visible range (440–780 nm), both the absorption spectra and fluorescence emission spectra of **F550/570** and **F650/670** are similar to those of common cyanine dyes, Cy3 and Cy5, respectively (26). The quantum yields (from three sets of measurements) of **F550/570** and **F650/670** are 0.16 ± 0.03 and 0.47 ± 0.06, respectively, compared with 0.11 ± 0.03 and 0.27 ± 0.04 for their corresponding precursors **3** and **4**. Therefore, the attachment of two adenosines and HDA linkers at the opposite ends of the cyanine cores increases their quantum yields, but has no apparent effects on other spectroscopic properties of the cyanine dye within the visible range.

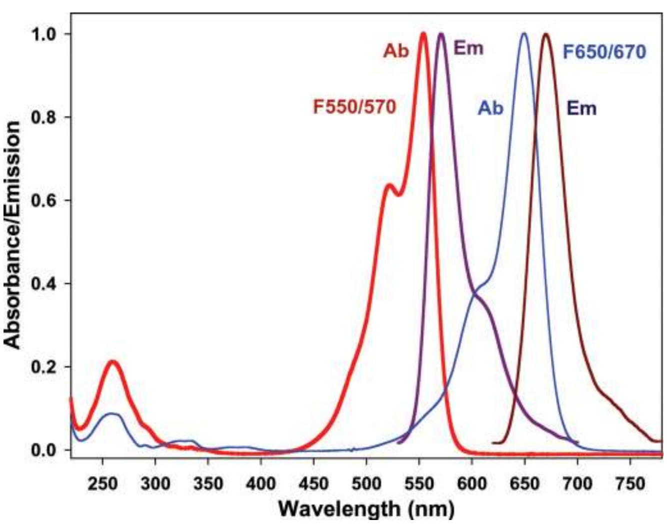


**Figure 3.** UV–visible absorption spectra (Ab) and fluorescence emission spectra (Em) of **F550/570** and **F650/670**. The spectra were measured in 20 mM phosphate buffer, pH 7.0. All spectra were normalized to 1 at their $\lambda_{max}$. The $\lambda_{max}$ difference between excitation and emission is 20 nm for both **F550/570** and **F650/670**.

## Fluorescent labeling of 5′ RNA by F550/570 and F650/670

Fluorescent labeling of 5′ RNA is achieved by simply including **F550/570** or **F650/670** in transcription solutions under the T7 class II promoter ϕ2.5 (18,19). One of the two adenosines within **F550/570** or **F650/670** initiates transcription, resulting in 5′ RNA labeling by the cyanine dyes. Although there are two identical adenosines within **F550/570** or **F650/670**, the probability of both adenosines initiating transcription to produce head-to-head joined RNA via **F550/570** or **F650/670** is low due to the high concentration ratios of **F550/570** (or **F650/670**) over transcribed RNA molecules (i.e. mM versus μM). To confirm the prediction, purified **F550/570-**RNA (TES33, $^{32}$P-labeled) was added to the transcription solution in the absence of [α-$^{32}$P]ATP and **F550/570**. No head-to-head joined RNA dimer was observed by phosphorimaging after PAGE. Because neither **F550/570** nor **F650/670** contains a nucleoside 5′-triphosphate, the cyanine dyes cannot be incorporated into internal RNA positions by T7 RNA polymerase. Figure 4 shows 5′ RNA (TES33) labeling by **F550/570** and **F650/670**. Three parallel transcription experiments (with [α-$^{32}$P]ATP as the internal radiolabel) were carried out in the absence of the cyanine dyes (lane 1) or in the presence of **F550/570** (lane 2) or **F650/670** (lane 3). Phosphorimaging based on $^{32}$P (Figure 4A) revealed an additional slower RNA band in lanes 2 and 3. Fluorescence scanning of the same gel under the excitation with the 532 nm green laser (Figure 4B) shows only a single RNA band in lane 2, whose location overlaps with that of the upper band of lane 2 in Figure 4A. Under the excitation of a 633 nm red laser (Figure 4C), scanning of the same gel displays another single RNA band in lane 3, whose location superimposes with that of the upper band of lane 3 in Figure 4A. Taken together, the three different scannings of the same gel based on excitation by $^{32}$P (Figure 4A), 532 nm photons (Figure 4B) and 633 nm photons (Figure 4C) indicate fluorescent labeling of RNA by **F550/570** (lane 2) and **F650/670** (lane 3) during transcription. The labeling yields were 60 ± 5% and 35 ± 5% for **F550/570** and **F650/670**, respectively. Total RNA yields for **F550/570-** and **F650/670-**labeled RNA were 110 ± 30% and 90 ± 30% of the control RNA (in the absence of dye-AMP). In a different set of labeling experiments with varying RNA sizes (100–500 nt), 15 independent transcriptions gave labeling yields of 78 ± 3% and 55 ± 3% for **F550/570** and **F650/670**, respectively. The respective total RNA yields relative to the control RNA were 150 ± 30% and 110 ± 30%. Therefore, **F550/570** and **F650/670** appear to stimulate transcription initiation under the transcription



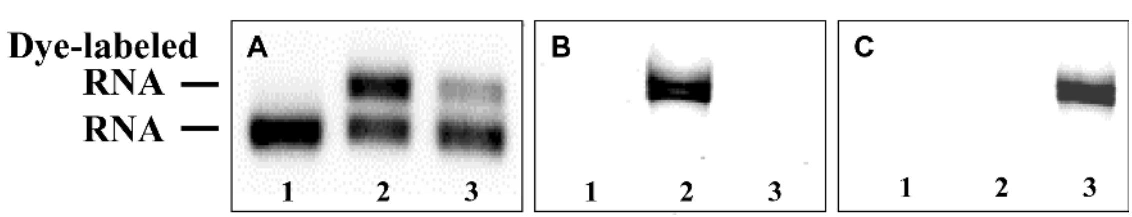


**Figure 4.** RNA fluorescent labeling by **F550/570** and **F650/670** under the T7 ϕ2.5 promoter (18,19). All RNA was also internally $^{32}$P-labeled by [α-$^{32}$P]ATP. After transcription, RNA samples were fractionated by PAGE. Lane 1, normal transcription; lanes 2 and 3, transcription in the presence of **F550/570** and **F650/670**, respectively. (**A**) $^{32}$P-phosphorimaging reveals total RNA bands in different transcription experiments. (**B**) Scanning of the same gel under the excitation of a 532 nm laser shows only **F550/570**-labeled RNA. (**C**) Under excitation with a 633 nm laser, only **F650/670**-labeled RNA is visible. The RNA sequence was that of a thioester-synthesizing ribozyme TES33, 92 nt (24). RNAs from ∼5 μl transcription were used for the gel.

conditions. In a typical experiment, ∼20 μg of dye-labeled RNA can be prepared from 100 μl transcription.

Since no transcription-based methods would produce 100% labeled RNA, isolation of labeled RNA from unlabeled (normal) RNA may be required for its applications. Owing to their relatively large sizes, **F550/570**- and **F650/670**-labeled RNA displays significant migration retardation (5–6 nt difference) by PAGE. This added property of **F550/570**- and **F650/670**-labeled RNA may be exploited to achieve high purity levels of fluorescent RNA by PAGE. To establish the RNA size-PAGE resolution relationship, five different sizes of RNA (100, 200, 300, 400 and 500 nt) were labeled by both $^{32}$P and **F550/570** (**F650/670**) and run 30 cm on a large sequencing gel ($42 \times 35 \times 0.08$ cm$^3$). As shown in Figure 5A, gel-running time varied from ∼4 h for an RNA of 100 nt to ∼18 h for the 500 nt RNA. Separation between dye-labeled RNA and unlabeled RNA ranged from 12 to 3 mm when RNA increased from 100 to 500 nt (Figure 5B). Therefore, **F550/570**- and **F650/670**-labeled RNA (up to 500 nt, depending on the skill of the experimenter) can be separated from unlabeled RNA by 8% PAGE. In one experiment, we purified an **F550/570**-labeled 120-nt RNA to >95% purity using 8% denaturing PAGE ($42 \times 35 \times 0.08$ cm$^3$) after running for 4 h at 45 V/cm.

### Replacement of [γ-$^{32}$P]ATP by F550/F570 in RNA reaction site mapping

Investigation of RNA structure/function/mechanism frequently requires the use of [5′-$^{32}$P]RNA (27–29). However, it may be difficult to phosphorylate some RNA by [γ-$^{32}$P]ATP and polynucleotide kinase (PNK) due to the structure of RNA. As an example, a recently isolated ribozyme (ACT3) from our laboratory poses such a problem. ACT3 is a ribozyme that catalyzes the formation of aminoacylated RNA from aminoacyl thioesters of CoA (25). Attempts to label the 5′ HO-ACT3 by [γ-$^{32}$P]ATP and PNK gave very poor (<2%) labeling yields due to the 5′ recessed structure (Figure 6A). Here, we demonstrate that 5′ **F550/570**-labeled RNA can be used to map the reaction site within the ribozyme.

BiocytinCoA-reacted RNA, which was 5′ end-labeled by **F550/570**, was first treated with lead acetate to generate all possible single-cut RNA fragments. The resulting RNA sample contained both biocytin-tagged RNA fragments and normal RNA fragments. After Neutravidin affinity chromatography, only biocytin-tagged RNA fragments would be retained on the column. Analysis of the eluted RNA sample by PAGE and **F550/570**-based fluorimaging should reveal the location of the reactive site within the ribozyme. Figure 6B shows the fluorescence scanning image of RNA fragments eluted from the Neutravidin column. Figure 6C is the profile of **F550/570** fluorescence intensity from Figure 6B. The gel indicates that RNA fragments shorter than C51 (from the 5′ end) were completely missing from the affinity column, while all the fragments longer than C51 were present. The result is schematically interpreted in Figure 6D. The C51 RNA fragment (with 5′ **F550/570** as well) thus contained the reaction site at a 2′ OH group. Since lead-induced RNA hydrolysis requires the presence of a free 2′ OH group, the actual reaction site is the 2′ OH group of U50, which agrees with the results obtained by reverse transcriptase-catalyzed primer extension, HPLC analysis and MS analysis (25).

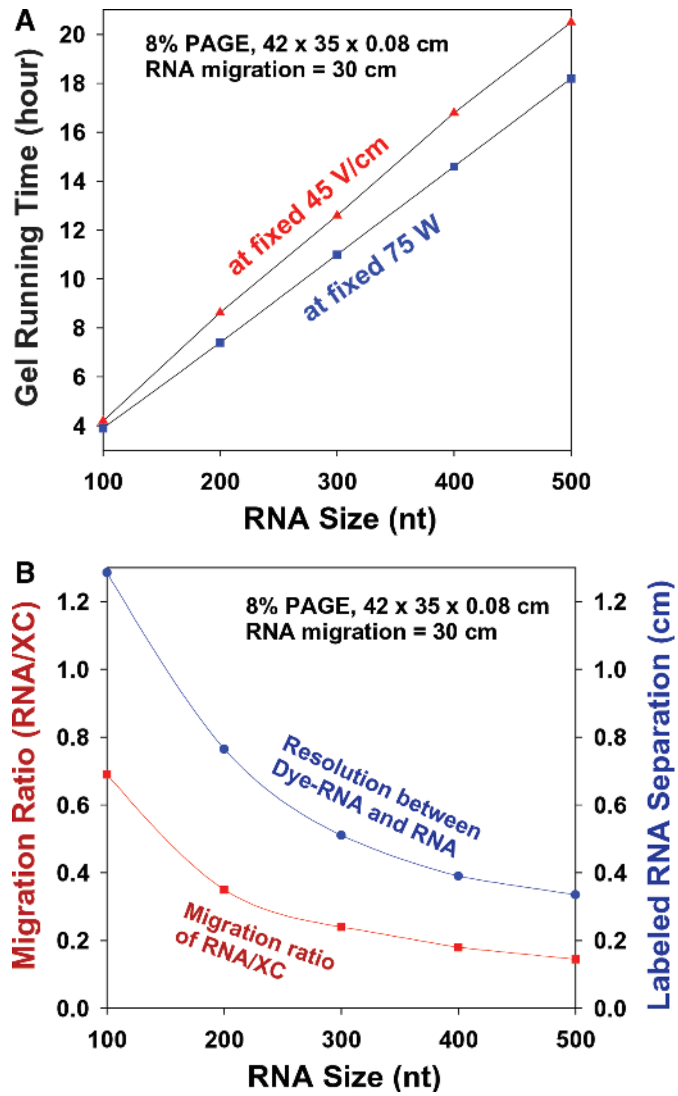


**Figure 5.** Resolution of dye-labeled RNA of different sizes by 8% PAGE ($42 \times 35 \times 0.08$ cm$^3$). Each RNA was run 30 cm from the origin under either constant voltage or constant wattage. (**A**) The relationship of RNA size and gel-running time under two different conditions. (**B**) Relative electrophoretic mobility of different RNA sizes to xylene cyanol (XC) and resolution between dye-labeled RNA and unlabeled RNA.

## DISCUSSION

Our approach for direct fluorescent labeling of RNA by **F550/570** and **F650/670** during transcription offers the following distinct advantages over the phosphoramidite chemistry method and post-transcriptional fluorescent labeling. First, site-specific RNA fluorescent labeling is achieved in a single step of transcription, greatly reducing the RNA sample handling time and RNA loss. Typically, fluorophore-labeled RNA can be made available in common laboratories within 2–4 h. Second, there is no apparent RNA size restriction; fluorescently labeled small and large RNAs can be prepared by the same transcription method with similar yields, purities and costs. The commonly used *in vitro* transcription under the T7 ϕ6.5 promoter produces G-initiated RNAs. The same RNA sequences can be used for fluorescence labeling under

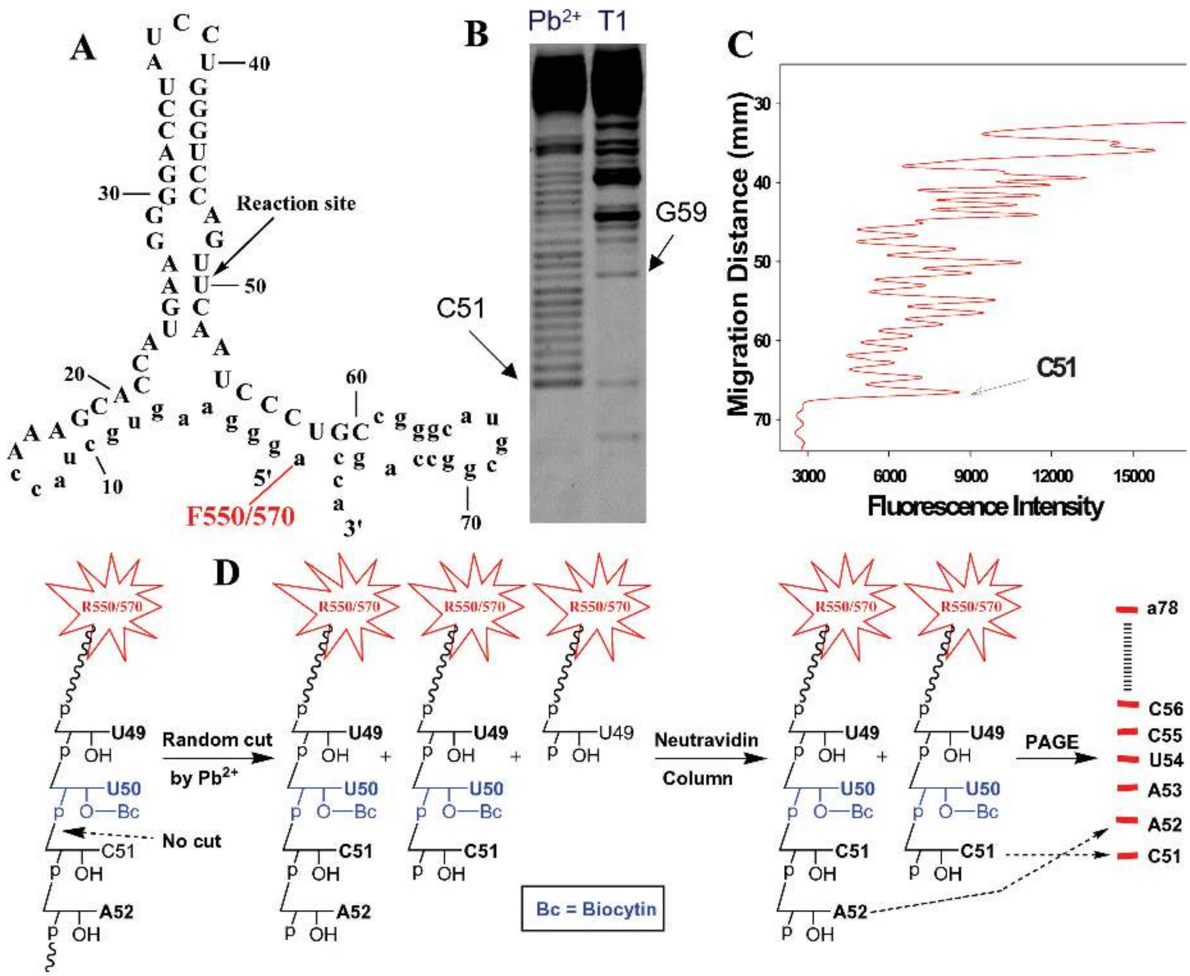


**Figure 6.** Ribozyme reaction site mapping by **F550/570**-labeled RNA. RNA from 10 µl transcription was used for the analysis. (**A**) The secondary structure of ACT3 (25). It is difficult to label the 5′ end by [γ-$^{32}$P]ATP and PNK due to its recessed 5′ end. (**B**) PAGE analysis of Neutravidin column-eluted RNA fragments (lane 1), along with an RNase T1-digested ladder of the same **F550/570**-labeled RNA. RNA fragments were generated by partial lead hydrolysis of biocytinCoA-reacted RNA (**F550/570**-labeled). After electrophoresis, the gel was scanned directly by an Amersham Typhoon phosphorimager under the excitation of a 532 nm laser. (**C**) Fluorescence intensity profile of lane 1 in (B). (**D**) An illustration of the reaction site mapping. Controlled lead-induced RNA hydrolysis randomly cuts the RNA to all possible fragments, except for the reactive site where the 2′ OH is blocked by biocytin. The eluted RNA sample from Neutravidin chromatography contains all biocytin-tagged fragments, C51 and above. None of the untagged RNA fragments (U49 and below) is retained by the column. Therefore, PAGE analysis and **F550/570**-based phosphorimaging can detect all RNA fragments equal to or longer than C51. The reaction site is one nucleotide below C51, i.e. U50.

the T7 ϕ2.5 promoter by adding an extra A before the first G. Third, **F550/570** and **F650/670** are chemically stable, allowing laboratories to maintain steady stocks without constant purchase of fresh supplies. The current finding will make site-specifically fluorophore-labeled RNA readily available for a variety of applications in biochemistry, structural biology and nucleic acids-based clinical diagnostics. In particular, fluorophore-labeled large RNAs prepared by the current method may be appealing to biochemists and structural biologists to investigate RNA structure, folding and mechanism by various fluorescence techniques such as fluorescence resonance energy transfer (6–9,13) and single-molecule kinetics (10,15,30). Without an apparent restriction on RNA sequence (except for the 5′ AG) and size, the described fluorescent labeling by **F550/570** and **F650/670** can be easily applied to large RNAs such as the group I and group II introns, the RNase P RNA, spliceosomal RNAs, ribosomal RNAs and artificially selected functional RNAs (aptamers and ribozymes).

PNK-catalyzed phosphorylation by [γ-$^{32}$P]ATP is a common procedure to prepare [5′-$^{32}$P]RNA that is required in various studies of structure/function/mechanism (27–29). However, such a $^{32}$P-based RNA labeling method may present a series of problems for the experimenter. First, $^{32}$P radioactivity quickly diminishes with time due to its short half-life. In addition, RNA labeling efficiency by [γ-$^{32}$P]ATP actually decreases much faster than the radiodecay of $^{32}$P, probably due to ATP damage caused by strong $^{32}$P radioactivity. Therefore, usable [γ-$^{32}$P]ATP has an even shorter half-life (<14 days). Frequent supply of fresh [γ-$^{32}$P]ATP is necessary for efficient 5′ RNA labeling by $^{32}$P and PNK. Unless it is used by several experimenters in a sizable laboratory or shared among different laboratories, a substantial amount of [γ-$^{32}$P]ATP is wasted due to its fast radiodecay. Second, [5′-$^{32}$P]RNA may slowly lose its function during storage as a result of structural damage by its $^{32}$P radioactivity. Accordingly, it may be necessary to frequently prepare freshly $^{32}$P-labeled RNA before a previous preparation is fully consumed. Third, some RNA (such as the one shown in Figure 6A) may present difficulties for efficient labeling by PNK and [γ-$^{32}$P]ATP. Finally, $^{32}$P is a source of radio-hazard. Its use requires user training and strict workplace safety regulations.

Our newly developed **F550/570** and **F650/670** offer solutions to the above [γ-$^{32}$P]ATP-based RNA labeling problems. Regardless of RNA structure, the 5′ end of RNA can be readily labeled by **F550/570** and **F650/670**, if the RNA has AG at its 5′ end. If the subject RNA does not possess a 5′ AG sequence, AG can be added to the 5′ end for the purpose of facilitating 5′ fluorescent labeling by **F550/570** or **F650/670**. With phosphorimagers/fluorimagers becoming widely accessible, the RNA-labeling advantages offered by **F550/570** and **F650/670** over traditional $^{32}$P-based methods may be fully realized.

The cyanine dye-AMP conjugates **F550/570** and **F650/670** described in this report have been made available by AdeGenix Inc. (Monrovia, CA). Detailed application notes can be found at www.adegenix.com.

## ACKNOWLEDGEMENTS

We would like to thank Peter Butko and George Santangelo for the use of fluorometer and phosphorimager, respectively. This work was partially supported by a NASA grant NAG5-10668. Funding to pay the Open Access publication charges for this article was provided by NASA.

## REFERENCES

1. Tuschl,T., Gohlke,C., Jovin,T.M., Westhof,E. and Eckstein,F. (1994) A three-dimensional model for the hammerhead ribozyme based on fluorescence measurements. *Science*, **266**, 785–789.
2. Qin,P.Z. and Pyle,A.M. (1997) Stopped-flow fluorescence spectroscopy of a group II intron ribozyme reveals that domain 1 is an independent folding unit with a requirement for specific $Mg^{2+}$ ions in the tertiary structure. *Biochemistry*, **36**, 4718–4730.
3. Walter,N.G., Hampel,K.J., Brown,K.M. and Burke,J.M. (1998) Tertiary structure formation in the hairpin ribozyme monitored by fluorescence resonance energy transfer. *EMBO J.*, **17**, 2378–2391.
4. Singh,K.K., Parwaresch,R. and Krupp,G. (1999) Rapid kinetic characterization of hammerhead ribozymes by real-time monitoring of fluorescence resonance energy transfer (FRET). *RNA*, **5**, 1348–1356.
5. Walter,N.G. and Burke,J.M. (2000) Fluorescence assays to study structure, dynamics, and function of RNA and RNA–ligand complexes. *Methods Enzymol.*, **317**, 409–440.
6. Klostermeier,D. and Millar,D.P. (2002) Time-resolved fluorescence resonance energy transfer: a versatile tool for the analysis of nucleic acids. *Biopolymers*, **61**, 159–179.
7. Klostermeier,D. and Millar,D.P. (2001) RNA conformation and folding studied with fluorescence resonance energy transfer. *Methods*, **23**, 240–254.
8. Walter,N.G., Harris,D.A., Pereira,M.J. and Rueda,D. (2002) In the fluorescent spotlight: global and local conformational changes of small catalytic RNAs. *Biopolymers*, **61**, 224–242.
9. Walter,N.G. (2001) Structural dynamics of catalytic RNA highlighted by fluorescence resonance energy transfer. *Methods*, **25**, 19–30.
10. Kim,H.D., Nienhaus,G.U., Ha,T., Orr,J.W., Williamson,J.R. and Chu,S. (2002) $Mg^{2+}$-dependent conformational change of RNA studied by fluorescence correlation and FRET on immobilized single molecules. *Proc. Natl Acad. Sci. USA*, **99**, 4284–4289.
11. Sekella,P.T., Rueda,D. and Walter,N.G. (2002) A biosensor for theophylline based on fluorescence detection of ligand-induced hammerhead ribozyme cleavage. *RNA*, **8**, 1242–1252.
12. Klostermeier,D., Sears,P., Wong,C.H., Millar,D.P. and Williamson,J.R. (2004) A three-fluorophore FRET assay for high-throughput screening of small-molecule inhibitors of ribosome assembly. *Nucleic Acids Res.*, **32**, 2707–2715.
13. Lilley,D.M. (2004) Analysis of global conformational transitions in ribozymes. *Methods Mol. Biol.*, **252**, 77–108.
14. Rueda,D., Bokinsky,G., Rhodes,M.M., Rust,M.J., Zhuang,X. and Walter,N.G. (2004) Single-molecule enzymology of RNA: essential functional groups impact catalysis from a distance. *Proc. Natl Acad. Sci. USA*, **101**, 10066–10071.
15. Xie,Z., Srividya,N., Sosnick,T.R., Pan,T. and Scherer,N.F. (2004) Single-molecule studies highlight conformational heterogeneity in the early folding steps of a large ribozyme. *Proc. Natl Acad. Sci. USA*, **101**, 534–539.
16. Qin,P.Z. and Pyle,A.M. (1999) Site-specific labeling of RNA with fluorophores and other structural probes. *Methods*, **18**, 60–70.
17. Czworkowski,J., Odom,O.W. and Hardesty,B. (1991) Fluorescence study of the topology of messenger RNA bound to the 30S ribosomal subunit of *Escherichia coli*. *Biochemistry*, **30**, 4821–4830.
18. Huang,F. (2003) Efficient incorporation of CoA, NAD and FAD into RNA by *in vitro* transcription. *Nucleic Acids Res.*, **31**, e8.
19. Huang,F., Wang,G., Coleman,T. and Li,N. (2003) Synthesis of adenosine derivatives as transcription initiators and preparation of 5′ fluorescein- and biotin-labeled RNA through one-step *in vitro* transcription. *RNA*, **9**, 1562–1570.
20. Southwick,P.L., Carins,J.G., Ernst,L.A. and Waggoner,A.S. (1988) One pot Fischer synthesis of (2,3,3-trimethyl-3H-indol-5-yl)acetic acid. Derivatives as intermediates for fluorescent biolabels. *Org. Prep. Proceed. Int.*, **20**, 279–284.
21. Southwick,P.L., Ernst,L.A., Tauriello,E.W., Parker,S.R., Mujumdar,R.B., Mujumdar,S.R., Clever,H.A. and Waggoner,A.S. (1990) Cyanine dye labeling reagents—carboxymethylindocyanine succinimidyl esters. *Cytometry*, **11**, 418–430.
22. Karstens,T. and Kobs,K. (1980) Rhodamine B and Rhodamine 101 as reference substance for fluorescence quantum yield measurements. *J. Phys. Chem.*, **84**, 1871–1872.
23. Vincett,P.S., Voigt,E.M. and Rieckhoff,K.E. (1971) Phosphorescence and fluorescence of phthalocyanines. *J. Chem. Phys.*, **55**, 4131–4140.
24. Coleman,T.M. and Huang,F. (2002) RNA-catalyzed thioester synthesis. *Chem. Biol.*, **9**, 1227–1236.
25. Li,N. and Huang,F. (2004) Ribozyme-catalyzed aminoacylation from CoA thioesters. *Biochemistry*, in press.
26. Mujumdar,R.B., Ernst,L.A., Mujumdar,S.R., Lewis,C.J. and Waggoner,A.S. (1993) Cyanine dye labeling reagents: sulfoindocyanine succinimidyl esters. *Bioconjug. Chem.*, **4**, 105–111.
27. Celander,D.W. and Cech,T.R. (1991) Visualizing the higher order folding of a catalytic RNA molecule. *Science*, **251**, 401–407.
28. Sclavi,B., Sullivan,M., Chance,M.R., Brenowitz,M. and Woodson,S.A. (1998) RNA folding at millisecond intervals by synchrotron hydroxyl radical footprinting. *Science*, **279**, 1940–1943.
29. Swisher,J., Duarte,C.M., Su,L.J. and Pyle,A.M. (2001) Visualizing the solvent-inaccessible core of a group II intron ribozyme. *EMBO J.*, **20**, 2051–2061.
30. Zhuang,X. and Rief,M. (2003) Single-molecule folding. *Curr. Opin. Struct. Biol.*, **13**, 88–97.